Solving the Air Conflict Resolution Problem under Uncertainty using an Iterative Bi-Objective Mixed Integer Programming Approach

Thibault Lehouillier, Ilies Nasri, Jérémy Omer, François Soumis, Guy Desaulniers

Solving the Air Conflict Resolution Problem under Uncertainty as an Iterative Bi-Objective Mixed Integer Linear Program*

Thibault Lehouillier[1,2], Moncef Ilies Nasri[1,2], Jérémy Omer[3], François Soumis[1,2], and Guy Desaulniers[1,2]

[1]*Group for Research in Decision Analysis, HEC Montréal, 3000, chemin de la Côte-Sainte-Catherine, Montréal (Quebec) Canada, H3T 2A7*
[2]*École Polytechnique Montréal, 2900 Boulevard Édouard-Montpetit, Montréal (Quebec) Canada, H3T 1J4*
[3]*Institut de Recherche Mathématique de Rennes & INSA de Rennes, Rennes, France*

Abstract

In this paper, we tackle the aircraft conflict resolution problem under uncertainties. We consider errors due to the wind effect, the imprecision on the aircraft speed prediction, and the delay in the execution of maneuvers. Using a geometrical approach, we derive an analytical expression for the minimum distance between aircraft, along with the corresponding probability of conflict. These expressions are incorporated into an existing deterministic model for conflict resolution. This model solves the problem as a maximum clique of minimum weight in a graph whose vertices represent possible maneuvers and where edges link conflict-free maneuvers of different aircraft. We then present a solution procedure focusing on two criteria, namely fuel efficiency and the probability of re-issuing maneuvers in the future: we iteratively generate solutions of the Pareto front to provide the controller with a set of possible solutions where he/she can choose the one corresponding the most to his/her preferences. Intensive Monte-Carlo simulations validate the expressions derived for the minimum distance and the probability of conflict. Computational results highlight that up to 10 different solutions for instances involving up to 35 aircraft are generated within three minutes.

Keywords: Air Traffic Management, Air Traffic Control, Mixed Integer Linear Programming, Uncertainties, Multi-Objective Programming

1 Introduction

1.1 Automating air traffic control

In the current air traffic management (ATM) organization, the air traffic control (ATC) is in charge of maintaining safety. To this end, controllers monitor the traffic to ensure the separation between all aircraft at all times. A projected loss of separation between two aircraft is called a *conflict* and must be solved by the controller. To this end, avoidance maneuvers are issued to the pilots of the involved aircraft to prevent the loss of separation. Maintaining safety in the

 Doi:10.1287/trsc.2016.0714

airspace is a challenging task, especially in a context of increasing traffic. Indeed, the latest long-term forecast published by EUROCONTROL states that the traffic demand will increase by 20% to 80% between 2012 and 2035 (EUROCONTROL, 2013). Besides, a simulation-based study performed by Lehouillier et al. (2014) shows that for a 50% increase in traffic, the controllers in charge of busy sectors would have to solve 27 conflicts per hour on average. During the last decade a lot of research was conducted on the development of automated decision tools to help the controller. Such automated tools are recognized as key-components of future ATM systems like the Single European Sky ATM Research (see SESAR Joint Undertaking (2012)) project in Europe and the Next Gen(see Joint Planning and Development Office (2008) for details) program in the United States.

1.2 The air conflict resolution problem

One complex and central problem encountered in ATC is the air conflict resolution problem (CR). A conflict occurs when two aircraft are too close to each other regarding predefined horizontal and vertical separation distances of respectively 5NM and 1000ft. To solve a conflict, the controllers issue maneuvers that can consist of speed, heading or altitude changes. Given the current position, speed, acceleration and the predicted trajectory of a set of aircraft, the CR problem corresponds to identifying the conflict-free maneuvers that minimize a given cost function. The CR problem can be tackled following two different settings, namely deterministic and stochastic. The first one assumes that aircraft follow exact trajectory predictions, along with maneuvers applied without any errors. However, uncertainties are one of the reasons why ATC is a complicated task. The weather conditions, along with the incomplete knowledge of the physical characteristics of the aircraft and the imprecision during the communication and maneuver execution processes represent the main factors of uncertainty in ATC (Erzberger et al. (1997)). In this context, the uncertainties cause a perturbation of the trajectory, inducing cross and along-track errors in the prediction of the trajectory. The along-track error (or longitudinal error) is the distance between the predicted aircraft position and the projection of the actual aircraft position on the predicted trajectory. The cross-track error (or lateral error) corresponds to the distance between the actual aircraft position and the predicted trajectory. Figure 1 illustrates these errors. They can jeopardize the conflict resolution process. To tackle this issue, stochastic resolution methods aim at solving the CR problem while taking into account these perturbations.

Figure 1: Cross and along-track errors on an aircraft trajectory

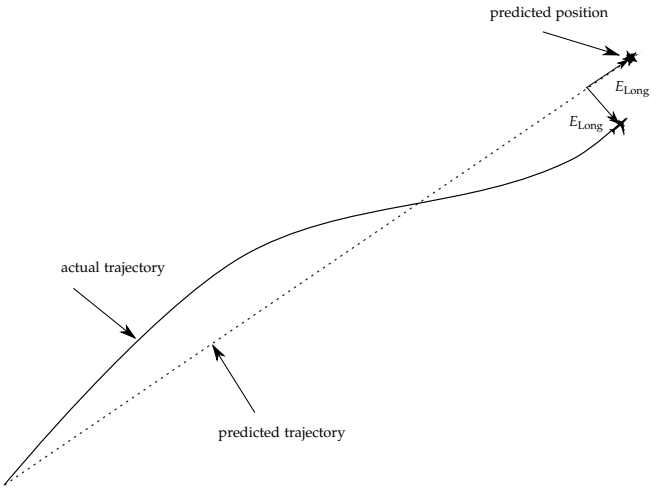

1.3 Literature review on the CR problem

The CR problem is one of the most widely studied problems in ATM. We provide a synthetic analysis of the studies that were most influential to our work, both in a deterministic and a stochastic setting.

A complete coverage of the existing literature on the deterministic CR problem may be found in the review performed in Martín-Campo (2010). Mixed integer linear and nonlinear programming are powerful theoretical frameworks for the study of CR. With the realistic restriction that the aircraft perform at most one maneuver at the initial time, Pallottino et al. (2002) exploit the geometry of the separation constraints to develop two mixed integer linear programs (MILPs) that allow either speed changes with constant headings or heading changes with constant speeds. Alonso-Ayuso et al. (2012) extend the model of Pallottino et al. (2002) by introducing continuous instead of instantaneous speed changes. More recently, Omer (2015) develops a MILP with a space discretization using only the points of interest for the conflict resolution.

Uncertainties can be gathered and modeled as having a global impact on the trajectory prediction. Ballin and Erzberger (1996) quantify the along-track error by comparing prediction and actual data for the Dallas Fort Worth Airport. Results highlight that for a time horizon shorter than 20 minutes, the error follows a normal distribution. Irvine (2002) develops an expression of the minimum distance and the corresponding probability of conflict using a geometrical approach. The author models cumulative cross and along track errors that are affected to each aircraft at the beginning of the observation. After applying this initial perturbation, aircraft are assumed to evolve in a deterministic environment. Uncertainties can also be divided into different categories than can be modeled more specifically. For instance, Lygeros and Prandini (2002) model the effect of the wind and the resulting FMS correction. Cole et al. (1998) and Schwartz et al. (2000) conduct statistical studies comparing predictions to actual data in the Denver area to derive the correlation structure of the wind. Chaloulos and Lygeros (2007) study the perturbations due to imprecisions in the speed and air temperature measures. The authors model the error as a normal distribution.

When the uncertainties become too complex to derive exact probability expressions, Monte-Carlo simulations are often performed. Prandini et al. (2000) use Monte-Carlo simulations to develop a model where the wind correlates the cross and along track errors.

1.4 Critical analysis and contribution statement

The literature review highlights that a lot of results have been established to solve the CR problem, both in the deterministic and the stochastic setting. Nevertheless, some features still need to be addressed. More specifically, we formulate three observations that we consider important when designing a resolution tool for the CR problem. The first one relies on the fact that robustness is critical in ATC. A large span of factors can have a dramatic impact on the conflict resolution. As a consequence, it is necessary to provide the controller with a tool as robust as possible. In other words, the controller needs to be ready to handle every possible situation. To this end, the mathematical framework in the developed decision tools needs to remain valid, whatever the hypotheses followed. Unfortunately, a lot of models lack of consistency when it comes to the modification of hypotheses, like the introduction of uncertainties, or other modeling features concerning the aircraft dynamics. For instance, the constraints in Pallottino et al. (2002) are linear when aircraft perform either a heading change or a speed change, but become nonlinear when both are performed. The second observation is related to the multi-objective nature of the CR problem. Indeed, focusing on only one objective, like the fuel consumption, or the delays, does not necessarily reflect all the aspects of the problem, nor does it respect the users' preferences. Several multi-objective approaches of the CR problem have been performed (Menon et al. (1999); Tomlin et al. (1998); Alonso-Ayuso et al.

(2016)), and research needs to be conducted in this direction. The last observation we formulate is that in conflict resolution the notion of optimality is subjective. Indeed, depending on the objective to optimize, the optimal solution is not necessarily far better than other good solutions. As a consequence, providing the controller with only one solution can be restrictive, depending on the context and the controller's preferences. Few work has been done on methods generating a set of solutions instead of a single solution. For instance, satisfycing game theory (see Stirling and Goodrich (1999) for a description of the theory) allows to generate a set of satisfycing solutions regarding two criteria representing the preferences of the players in terms of efficiency or resource consumption. Applications to ATC have been considered (see, e.g., Archibald et al. (2008)), but the hypotheses are quite restrictive, and the model suffers from a lack of computational power.

Our main contributions in our effort to provide an answer to the aforementioned remarks are twofold. First, we provide an analytical expression of the minimum distance and the probability of conflict in a context allowing complex uncertainties: the error in wind predictions is considered, along with the error on the aircraft speed prediction. We introduce the uncertainty on the delay in the execution of maneuvers, which to our knowledge has not been studied yet in the literature, although it is a reality in ATC. With this approach, we are able to cover a large span of uncertainties involved in ATC. Besides, these computations are fast compared to a simulation-based approach that can be more time consuming. Second, we model the CR problem as a bi-objective problem minimizing fuel consumption and the probability that the controller has to reissue maneuvers: we sequentially solve a mono-objective MILP. With this approach, we benefit from the powerful results yielded by MILPs, namely the guarantee of finding an optimal solution (if existing) in a short time, even for large and complex instances. Each iteration generates a solution that is immediately available to the user. The set of generated solutions is a tight approximation of the Pareto front of the solution. This method allows the user to choose which solution to apply within the generated set, depending on his/her preferences or other factors. The MILP used is taken from a preliminary study performed by Lehouillier et al. (2015b,a). It was chosen because it fully separates the modeling of the aircraft dynamics, maneuvers and cost function from the resolution process. As a consequence, the hypotheses considered do not jeopardize the validity of the proposed mathematical framework, and in particular the introduction of uncertainties. Besides, the fact that we are able to introduce uncertainties in the model from Lehouillier et al. (2015b) validates its robustness.

To evaluate the model, we first validate the computations derived for the probability of conflict by running Monte-Carlo simulations. We use several test beds generating 2000 random scenarios to verify the correctness of the developed theory. After the validation of the computations, we test our iterative resolution procedure by conducting intensive simulations on a benchmark of structured and random instances that are complex to solve. The aim of the experiments is to verify that our algorithm is able to provide the user with a set of solutions in a short period of time, while ensuring that separation is maintained in complex situations.

The organization of the paper will be as follows. We formulate the problem in Section 2. We describe the mathematical model to be adapted in Section 3. We detail the iterative optimization procedure used to generate the set of solutions in Section 4. The method is then tested and analyzed through intensive experiments described in Section 5.

2 Problem Formulation

2.1 Aircraft dynamics

As in the majority of the literature, we use a three-dimensional point-mass model for aircraft dynamics. This model establishes relationships between the different physical parameters of

each aircraft.

$$\frac{dp_x}{dt} = V\cos\gamma\cos\chi \quad (1)$$

$$\frac{dp_y}{dt} = V\cos\gamma\sin\chi \quad (2)$$

$$\frac{dp_z}{dt} = V\sin\gamma \quad (3)$$

$$\frac{d\gamma}{dt} = \frac{g_0}{V}(n\cos\phi - \cos\gamma) \quad (4)$$

$$\frac{d\chi}{dt} = \frac{g_0}{V}\frac{n\sin\phi}{\cos\gamma} \quad (5)$$

$$\frac{dV}{dt} = \frac{F_T - F_D}{m} - g_0\sin\gamma \quad (6)$$

The position of the aircraft is given by the coordinates (p_x, p_y, p_z) of its center of gravity in a local coordinate system, (p_x,p_y) being its coordinates in a horizontal plane and p_z its altitude. The aircraft flies at speed V and the angles χ, ϕ and γ correspond respectively to its heading, roll and pitch. F_T and F_D denote the norm of the thrust and drag forces respectively, m is the aircraft mass, n is the load factor and g_0 corresponds to the gravitational acceleration.

In this article, we make the assumption that aircraft are stabilized and follow a planar motion in a single flight level. Aircraft follow their trajectory with a stepwise constant acceleration. This assumption is realistic since it respects the time-continuity of speed, and it corresponds to a setting where maneuvers are performed smoothly.

2.2 Aircraft maneuvers

The maneuvers are horizontal maneuvers consisting in heading and speed changes. These maneuvers are performed dynamically in order to avoid a significant error in separation distance. Aircraft execute a speed or a heading change with a constant acceleration and turn angle, respectively, according to values extracted from Paielli (2003). Other types of maneuvers, i.e., flight level changes, could be considered without changing the validity of the mathematical resolution.

2.3 Aircraft trajectory recovery

We consider that aircraft follow a 4D contractual trajectory, which represents a compromise between the user's preferences and the capacity constraints of the network. The trajectories of the aircraft then have to meet time and space requirements over a sequence of 4D points. Noncompliance with this contract induces penalty fees to companies. As a consequence, it is important to make sure that, after resolving every conflict, every aircraft recovers its initial 4D trajectory. Ensuring a strict velocity control can be very costly and almost impossible in practice. Physicial recovery is required, whereas time recovery is optional, but it is favored by giving a penalty on the time shift between the 4D contract and the 4D trajectory after the maneuvers are performed.

2.4 Maneuver cost

The cost of a maneuver corresponds to the additional burnt to perform the maneuver, along with a time shift penalty. This measure serves as an indicator of the perturbation of the 4D trajectory induced by the executed maneuvers.

For a jet commercial aircraft f with constant altitude, the fuel consumption by time and distance unit is given by (7) and (8):

$$C_{t,f}\left(t, V_f(t)\right) = c_{1,f}\left(1 + \frac{V_f(t)}{c_{2,f}}\right) F_{T,f}(t) \tag{7}$$

$$C_{d,f}\left(t, V_f(t)\right) = \frac{C_{t,f}\left(t, V_f(t)\right)}{V_f(t)} \tag{8}$$

where $c_{1,f}$ and $c_{2,f}$ are numerical constants depending on the type of aircraft f that are extracted from the BADA performance tables EUROCONTROL (2011).

The time shift penalty is computed according to the method found in Omer and Farges (2013). The penalty corresponds to the extra fuel burnt to make up for the time shift.

2.5 Modeling the uncertainties

In this subsection, we detail the models used to describe the different uncertainties.

2.5.1 Error on wind prediction.

The aircraft are considered as flying within a wind field. Control commands are issued to reach the desired airspeed $\mathbf{v}_a$, while the control units monitoring the aircraft speed are ground-based. As a consequence, the groundspeed $\mathbf{v}_g$ can be linked to the airspeed. Let $\mathbf{w}(\mathbf{p}, t)$ denote the windspeed at position $\mathbf{p}$ at time t. We have that:

$$\mathbf{v}_g(t) = \mathbf{v}_a(t) + \mathbf{w}(\mathbf{p}(t), t) \tag{9}$$

The wind vector is decomposed in a *nominal* part corresponding to weather forecasts, and a *random* part describing the difference between the actual wind and its nominal part. The impact of the nominal wind of the aircraft dynamics is quite complex and was briefly studied in the literature. Most publications focus on the random part of the wind, and do not consider the nominal part. In this paper, we focus solely on the random wind.

The wind field is a set of random vectors $\mathbf{W}(\mathbf{p}, t)$ depending on the time and the point of space considered. Taking the wind into account complexifies the conflict resolution. Indeed, aircraft that are close from each other undergo highly correlated winds that will impact the conflict resolution. In this case, the error of prediction for the different aircraft become correlated. We follow the models presented in Lymperopoulos (2010). The authors simplify the computations performed in Cole et al. (1998) and Schwartz et al. (2000) in order to save execution time. The wind is stationary and isotropic, and each random vector $\mathbf{W}(\mathbf{p}, t)$ follows a zero-mean normal distribution such that the following conditions hold:

$$\mathbb{E}[\mathbf{W}(\mathbf{p}_1, t_1)] = 0, \forall t_1 \in \mathbb{R}_+, \forall \mathbf{p}_1 \in \mathbb{R}^2 \tag{10}$$

$$\mathbb{E}\left[\langle \mathbf{W}(\mathbf{p}_1, t_1) | \mathbf{W}(\mathbf{p}_2, t_2) \rangle\right] = 2f(t_1, \mathbf{p}_1, t_2, \mathbf{p}_2), \forall (t_1, t_2) \in \mathbb{R}_+^2, \forall (\mathbf{p}_1, \mathbf{p}_2) \in \mathbb{R}^4 \tag{11}$$

where f is the correlation function associated with the random wind developed in Cole et al. (1998).

We assume that the flight management system (FMS)compensates for the lateral errors, but does not correct the along-track errors. Indeed, the majority of commercial aircraft are equipped with 3D FMS which track only the cross-track errors.

2.5.2 Error on aircraft speed measures.

We consider the uncertainties due to the imprecision of speed and air temperature measures presented in Chaloulos and Lygeros (2007). These errors have an impact on the along-track

speed of the aircraft which is modeled as a zero-mean normal variable independent from the other aircraft. Since these two uncertainties are highly time-correlated, the authors assumed they were constant over time.

2.5.3 Delays in the execution of maneuvers.

We model uncertainties induced by delays in the execution of maneuvers, which to our knowledge has not been studied yet.

In the literature, models always assume that the performance of the maneuvers is instantaneous. However, there are several actions required before the maneuver can actually be performed. First, the automated decision tool has to provide the controller with a feasible solution. Then, the controller has to process the solution and then communicate the corresponding instructions to the pilots, before they can execute the maneuvers.

More formally, let T_i denote the maneuver delay for aircraft i. T_i is decomposed as follows:

- the time required for the resolution tool to provide the controller with a feasible solution, denoted T^s;
- the time during which the controller analyses the solution and communicates it to the different aircraft, denoted T^c;
- the time required for the pilot of aircraft i to execute the communicated maneuver, denoted T_i^p.

In other words T_i is the sum of a term shared by all aircraft including the solution process and the controller's communication, and a term depending on the pilot of i. Figure 2 summarizes the whole process resulting in the delay.

Figure 2: Structure of the maneuver delay

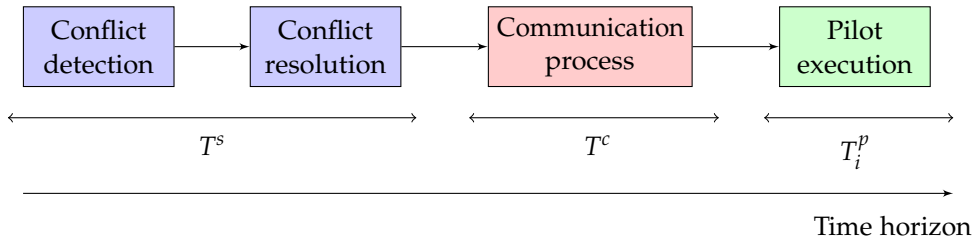

2.6 Analytical expressions of the minimum distance and the probability of conflict

2.6.1 Expression of Irvine (2002).

In this paragraph, we detail the work presented by Irvine (2002) which serves as the foundation for the method we use to derive the expression of the probability of conflict. In his article, Irvine models the global impact of the uncertainties and the resulting cross and along-track errors, instead of modeling each source of error differently.

Let A_i and A_j be two aircraft flying at a stabilized altitude at speed $\mathbf{v}_i$ and $\mathbf{v}_j$, respectively. Their trajectories intersect in O with a crossing angle θ_{ij}. Let $x_i(t)$ and $x_j(t)$ denote the curvilinear abscissa at time t of A_i and A_j in a coordinate system centered on O. The distance between the two aircraft can be computed as follows:

$$d(t)^2 = x_i(t)^2 + x_j(t)^2 - 2x_i(t)x_j(t)\cos\theta_{ij} \tag{12}$$

If $d(t)$ is replaced by the separation distance required between A_i and A_j, denoted d^{sep}, Equation (12) defines an ellipse in the coordinate system (O, x_i, x_j). The aircraft follow straight trajectories at constant speed, hence the set of points $\left(x_i(t), x_j(t)\right)_{t\geq 0}$ defines a straight line of slope

$$\frac{dx_j}{dx_i} = \frac{\frac{dx_j}{dt}}{\frac{dx_i}{dt}} = \frac{\mathbf{v}_j}{\mathbf{v}_i} = m \tag{13}$$

where m is the speed ratio between the two aircraft. If this line intersects the ellipse, then the aircraft are said to be in conflict. Figure 3 illustrates this condition.

Figure 3: Ellipse in the coordinate system (O, x_i, x_j)

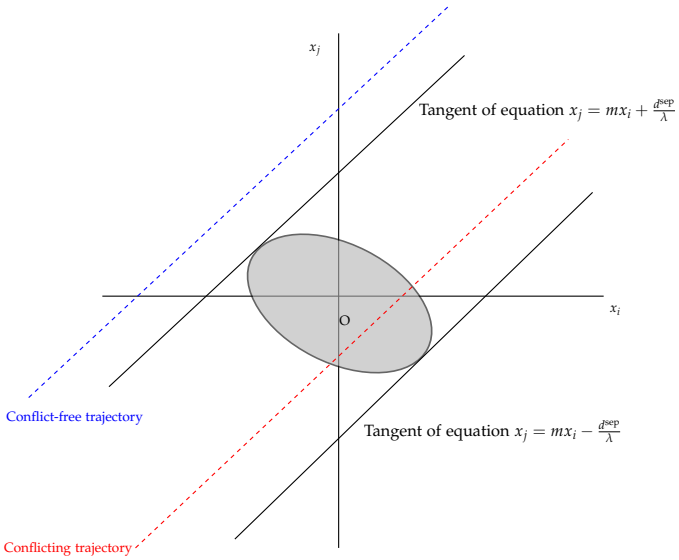

To derive an analytical expression of this condition, the author uses the two tangents of the ellipse that are parallel to the parametric line $\left(x_i(t), x_j(t)\right)_{t\geq 0}$. Their equations are given as follows:

$$x_j = mx_i \pm \frac{d^{\text{sep}}}{\lambda} \quad \text{where} \quad \lambda = \frac{\sin\theta_{ij}}{\sqrt{m^2 - 2m\cos\theta_{ij} + 1}}$$

The minimum distance between A_i and A_j in the deterministic case, denoted $d^{\min}$, can then be expressed as a function of the initial curvilinear abscissa of the two aircraft, x_i^0 and x_j^0.

$$d^{\min} = |\lambda(x_j^0 - mx_i^0)| \tag{14}$$

A_i and A_j are in conflict if and only if the minimum distance $d^{\min}$ is strictly less than the minimum separation distance allowed d^{sep}:

$$-d^{\text{sep}} < \lambda(x_j^0 - mx_i^0) < d^{\text{sep}}$$

Irvine then considers along-track errors and makes the assumption that within the range of along-track distances for which conflict is possible, the along-track error is approximately constant and that the aircraft flies with its predicted speed. This assumption is used to quantify

the cumulative along-track error between $t = 0$ and the instant where the two aircraft are the closest from each other in the deterministic case, denoted $t = \tau_{ij}$, given by

$$\tau_{ij} = \frac{(x_j^0 + mx_i^0)\cos\theta_{ij} - (x_i^0 + mx_j^0)}{||\mathbf{v}_i||(1 - 2m\cos\theta_{ij} + m^2)} \tag{15}$$

This value is chosen for τ_{ij} because the computation of the instant where the two aircraft are the closest from each other in the stochastic case is hard in practice. Consequently, deriving a handy formula of the probability of conflict would not be possible. Besides, considering τ_{ij} is a realistic assumption, since for the time intervals considered, the difference due to the approximation would be negligible.

The cumulative along-track error, denoted $\Delta L(\tau_{ij})$, follows a normal distribution $\mathcal{N}(0, \alpha_\sigma \tau_{ij})$, where α_σ is a constant. This error is applied to the initial position of the aircraft who then evolves in a entirely deterministic environment. This yields a new expression of the minimum distance in an uncertain setting, denoted $D^{\min}$.

$$D^{\min} = |\lambda(x_j^0 + \Delta L_j(\tau_{ij}) - mx_i^0 - m\Delta L_i(\tau_{ij}))| \tag{16}$$

$D^{\min}$ is the sum of a deterministic term with the sum of independent random variables. The sum of independent, normally distributed random variables is also normally distributed, with a mean equal to the sum of the means of the individual distributions, and variance equal to the sum of the variances of the individual distributions. As a consequence, we have that $D^{\min}$ follows a normal distribution of mean μ_d and variance σ_d^2 where

$$\mu_d = \lambda(x_j^0 - mx_i^0) \tag{17}$$

$$\sigma_d^2 = (\alpha_\sigma \tau)^2(1 + m)^2 \tag{18}$$

Irvine applies a similar reasoning for the impact of cross-track errors, but since we assume that the FMS compensates for these errors, in our article, we do not give any details about it.

The probability of conflict $\mathbb{P}_c$ is given by

$$\mathbb{P}_c = \mathbb{P}\big(|\lambda(x_j^0 + \Delta L_j(\tau) - mx_i^0 - m\Delta L_i(\tau))| < d^{\text{sep}}\big) \tag{19}$$

$$= \frac{1}{\sigma_d\sqrt{2\pi}} \int_{-d^{\text{sep}}-\mu_d}^{d^{\text{sep}}-\mu_d} \exp\Big(-\frac{u^2}{2\sigma_d^2}\Big)\,\mathrm{d}u \tag{20}$$

$$= \Phi\Big(\frac{d^{\text{sep}} - \mu_d}{\sigma_d}\Big) - \Phi\Big(\frac{-d^{\text{sep}} - \mu_d}{\sigma_d}\Big) \tag{21}$$

where Φ is the cumulative distribution function of the standard normal distribution.

2.6.2 Enriching the formula.

In this subsection, we modify the formula derived by Irvine by introducing the errors on the wind prediction, the speed measures, and the delay in the execution of maneuvers. These errors are independent.

We note these cumulative errors $\Delta X_i(\tau_{ij})$ and $\Delta X_j(\tau_{ij})$, respectively. They can be decomposed as follows:

$$\Delta X_i(\tau_{ij}) = \Delta W_i(\tau_{ij}) + \Delta S_i(\tau_{ij}) + \Delta D_i(\tau_{ij}) \tag{22}$$

$$\Delta X_j(\tau_{ij}) = \Delta W_j(\tau_{ij}) + \Delta S_j(\tau_{ij}) + \Delta D_j(\tau_{ij}) \tag{23}$$

where $\Delta W_\cdot$, $\Delta S_\cdot$ and $\Delta D_\cdot$ denote the cumulative error due to the wind, the speed prediction and the maneuver delay, respectively. Subsections 2.5.1 and 2.5.2 yield the following expressions for

$\Delta W_.$ and $\Delta S_.$:

$$\Delta W_i(\tau_{ij}) = \frac{\langle \mathbf{W}|\mathbf{v}_i\rangle}{||\mathbf{v}_i||}\tau_{ij} \qquad \Delta S_i(\tau_{ij}) = \Upsilon_i \tau_{ij} \tag{24}$$

$$\Delta W_j(\tau_{ij}) = \frac{\langle \mathbf{W}|\mathbf{v}_j\rangle}{||\mathbf{v}_j||}\tau_{ij} \qquad \Delta S_j(\tau_{ij}) = \Upsilon_j \tau_{ij} \tag{25}$$

where Υ_i and Υ_j denote the error due to speed measures for A_i and A_j, respectively.

The cumulative along-track error due to the maneuver delay is slightly more complex to determine. For the sake of clarity, we give an illustrative example in Figure 4 where two aircraft A_i and A_j flying with a speed $\mathbf{v}_i^0$ and $\mathbf{v}_j^0$ have to perform a heading change of value θ_i and θ_j, respectively. They perform these maneuvers with a delay corresponding to random variables denoted T_i and T_j, respectively.

Figure 4: Illustration of a maneuver delay for two aircraft performing heading changes

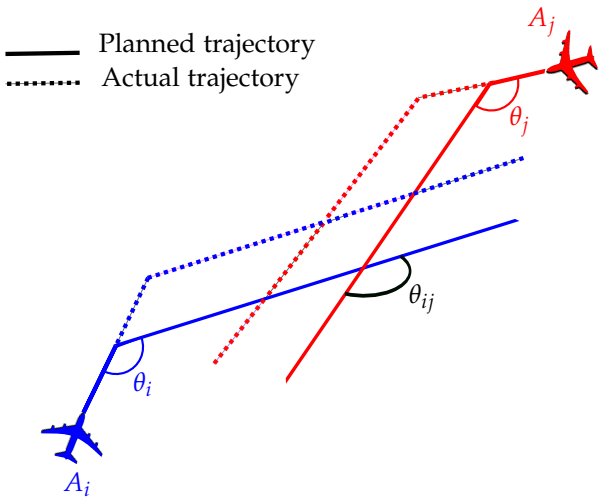

Figure 4 highlights that the crossing point of the aircraft trajectories was changed due to the delay in the execution of the maneuvers. As a consequence, there is a difference between the new initial curvilinear abscissas $\tilde{x}_i^0$ and $\tilde{x}_j^0$ and the ones in the deterministic setting x_i^0 and x_j^0. This difference, denoted ΔD_i^0 and ΔD_j^0, is computed as follows:

$$\Delta D_i^0 = T_i||\mathbf{v}_i^0|| - T_i||\mathbf{v}_i^0||\cos\theta_i - \frac{T_j||\mathbf{v}_j^0||\sin\theta_j}{\sin\theta_{ij}} - \frac{T_i||\mathbf{v}_i^0||\sin\theta_i\cos\theta_{ij}}{\sin\theta_{ij}} \tag{26}$$

$$\Delta D_j^0 = T_j||\mathbf{v}_j^0|| - T_j||\mathbf{v}_j^0||\cos\theta_j - \frac{T_i||\mathbf{v}_i^0||\sin\theta_i}{\sin\theta_{ij}} - \frac{T_j||\mathbf{v}_j^0||\sin\theta_j\sin\theta_{ij}}{\sin\theta_{ij}} \tag{27}$$

If $t < T_i$ then A_i has not started its maneuver yet and flies at speed $\mathbf{v}_i^0$. If $t \geq T_i$ then A_i has flown during T_i at speed $\mathbf{v}_i^0$ before changing its speed to $\mathbf{v}_i$. Since after T_i, aircraft A_i flies at speed v_i like it is supposed to, the cumulative along-track error due to the delay T_i until τ_{ij} is in fact cumulated on the interval $]0, T_i]$. The value of this error is derived by

$$\Delta D_i(T_i) = T_i(||\mathbf{v}_i^0|| - \mathbf{v}_i) \tag{28}$$

Variables $\Delta D_i(\tau_{ij})$ and $\Delta D_j(\tau_{ij})$ are derived with

$$\Delta D_i(\tau_{ij}) = \Delta D_i(T_i) + \Delta D_i^0 \tag{29}$$
$$\Delta D_j(\tau_{ij}) = \Delta D_j(T_j) + \Delta D_j^0 \tag{30}$$

yielding the following expressions:

$$\Delta D_i(\tau_{ij}) = 2T_i||\mathbf{v}_i^0|| - T_i\mathbf{v}_i - T_i||\mathbf{v}_i^0||\cos\theta_i - \frac{T_j||\mathbf{v}_j^0||\sin\theta_j}{\sin\theta_{ij}} - \frac{T_i||\mathbf{v}_i^0||\sin\theta_i\cos\theta_{ij}}{\sin\theta_{ij}} \tag{31}$$

$$\Delta D_j(\tau_{ij}) = 2T_j||\mathbf{v}_j^0|| - T_j\mathbf{v}_j - T_j||\mathbf{v}_j^0||\cos\theta_j - \frac{T_i||\mathbf{v}_i^0||\sin\theta_i}{\sin\theta_{ij}} - \frac{T_j||\mathbf{v}_j^0||\sin\theta_j\cos\theta_{ij}}{\sin\theta_{ij}} \tag{32}$$

To derive the new expression of the minimum distance between aircraft A_i and A_j, we aggregate the errors $\Delta X_i(\tau_{ij})$ and $\Delta X_j(\tau_{ij})$ into

$$D^{\min} = \left|\lambda\Big(x_j^0 + \Delta X_j(\tau_{ij})\Big) - m\Big(x_i^0 + \Delta X_i(\tau_{ij}\Big)\right| \tag{33}$$

$$\begin{aligned} &= \Bigg|\lambda\Big(\big(x_j^0 + \Delta W_j(\tau_{ij}) + \Delta S_j(\tau_{ij}) + \Delta D_j(\tau_{ij})\big) \\ &\quad - m\big(x_i^0 + \Delta W_i(\tau_{ij}) + \Delta S_i(\tau_{ij}) + \Delta D_i(\tau_{ij})\big)\Big)\Bigg| \end{aligned} \tag{34}$$

We simplify Equation (34) in order to determine an approximation of the distribution of variable $D^{\min}$.

In order to derive an analytical expression of the probability, we perform the computation with the hypothesis of a constant wind, which modifies the along-track speed of an aircraft flying at speed $\mathbf{v}$ by a factor $\frac{\langle \mathbf{w}|\mathbf{v}\rangle}{||\mathbf{v}||}$. This assumption seems reasonable since the considered intervals of detection and resolution are quite small and the wind is highly time-correlated. The terms related to the wind then correspond to

$$\begin{aligned} \Delta W_j(\tau_{ij}) - m\Delta W_i(\tau_{ij}) = {} & T_j\frac{\langle \mathbf{W}|\mathbf{v}_j^0\rangle}{||\mathbf{v}_j^0||} + (\tau_{ij} - T_j)\frac{\langle \mathbf{W}|\mathbf{v}_j\rangle}{\mathbf{v}_j} \\ & - m\left(T_i\frac{\langle \mathbf{W}|\mathbf{v}_i^0\rangle}{||\mathbf{v}_i^0||} + (\tau_{ij} - T_i)\frac{\langle \mathbf{W}|\mathbf{v}_i\rangle}{||\mathbf{v}_i||}\right) \end{aligned} \tag{35}$$

We approximate T_i and T_j by the mean of their distribution μ_{T_i} and μ_{T_j} in the quadratic terms, in order to find the analytical expression of the probability of conflict. This approximation is acceptable, since in Section 5 we use a distribution of T_i where the standard deviation is small compared to the mean. Equation (35) can be rewritten:

$$\begin{aligned} \Delta W_j(\tau_{ij}) - m\Delta W_i(\tau_{ij}) = {} & \left\langle \mathbf{W}\middle| \mu_{T_j}\frac{\mathbf{v}_j^0}{||\mathbf{v}_j^0||} + (\tau_{ij} - \mu_{T_j})\frac{\mathbf{v}_j}{||\mathbf{v}_j||} \right. \\ & \left. - m\mu_{T_i}\frac{\mathbf{v}_i^0}{||\mathbf{v}_i^0||} - m(\tau_{ij} - \mu_{T_i})\frac{\mathbf{v}_i}{||\mathbf{v}_i||}\right\rangle \end{aligned} \tag{36}$$

$$= \langle \mathbf{W}|\mathbf{u}\rangle \tag{37}$$

The terms involving the error on speed prediction can be simplified into

$$\Delta S_j(\tau_{ij}) - m\Delta S_i(\tau_{ij}) = \mathrm{Y}_j\tau_{ij} - m\mathrm{Y}_i\tau_{ij} \tag{38}$$
$$= \tau_{ij}(\mathrm{Y}_j - m\mathrm{Y}_i) \tag{39}$$

The terms related to the maneuver delay correspond to

$$\Delta D_j(\tau_{ij}) - m\Delta D_i(\tau_{ij}) = r_jT_j - mr_iT_i \tag{40}$$

where

$$r_j = ||\mathbf{v}_j|| - ||\mathbf{v}_j^0||\cos\theta_j + \frac{||\mathbf{v}_j^0||\sin\theta_j}{\tan\theta_{ij}} + \frac{m||\mathbf{v}_j^0||\sin\theta_j}{\sin\theta_{ij}}$$
$$r_i = ||\mathbf{v}_i|| - ||\mathbf{v}_i^0||\cos\theta_i + \frac{||\mathbf{v}_i^0||\sin\theta_i}{\tan\theta_{ij}} + \frac{||\mathbf{v}_i^0||\sin\theta_i}{m\sin\theta_{ij}}$$

Equations (35), (39) and (40) yield a simplified expression for $D^{\min}$:

$$D^{\min} = \left|\lambda(x_j^0 - mx_i^0) + \lambda\big((\mathrm{Y}_j - m\mathrm{Y}_i)\tau_{ij} + r_jT_j - mr_iT_i + \langle\mathbf{W}|\mathbf{u}\rangle\big)\right| \tag{41}$$

Equation (41) expresses $D^{\min}$ as a deterministic term $\lambda\big(x_j^0 - mx_i^0\big)$, added with the sum of the following independent random variables

- $(\mathrm{Y}_j - m\mathrm{Y}_i)\tau_{ij} \sim \mathcal{N}\big(0, (1+m)\sigma_{\mathrm{Y}}\tau_{ij}\big)$;
- $r_jT_j \sim \mathcal{N}(r_j\mu_{T_j}, r_j\sigma_{T_j})$;
- $-mr_iT_i \sim \mathcal{N}(-mr_i\mu_{T_i}, mr_i\sigma_{T_i})$;
- $\langle\mathbf{W}|\mathbf{u}\rangle \sim \mathcal{N}(0, \sigma_{\mathbf{W}}||\mathbf{u}||)$.

$D_{\min}$ follows a normal distribution of mean μ_D and variance σ_D^2 given by

$$\mu_D = \lambda\big((x_j^0 + r_j\mu_{T_j}) - m(x_i^0 + mr_i\mu_{T_i})\big) \tag{42}$$
$$\sigma_D^2 = \lambda^2\big(\sigma_{\mathrm{Y}}^2(1+m)^2\tau_{ij}^2 + (mr_i\sigma_{T_i})^2 + (r_j\sigma_{T_j})^2 + (\sigma_{\mathbf{W}}||\mathbf{u}||)^2\big) \tag{43}$$

The probability of A_i and A_j being in conflict corresponds to the probability of the event $|D^{\min}| < d^{\mathrm{sep}}$:

$$\mathbb{P}(|D^{\min}| < d^{\mathrm{sep}}) = P(-d^{\mathrm{sep}} < D^{\min} < d^{\mathrm{sep}})$$
$$= \Phi\Big(\frac{d^{\mathrm{sep}} - \mu_D}{\sigma_D}\Big) - \Phi\Big(\frac{-d^{\mathrm{sep}} - \mu_D}{\sigma_D}\Big)$$

3 Deterministic Model

In this section, we describe the resolution method developed by Lehouillier et al. (2015b,a) that will serve as a foundation for the optimization procedure presented in Section 4. The main idea is to model the CR problem as a maximum clique of minimum weight problem. To this end, we build a graph whose vertices represent maneuvers for the different aircraft, and where edges link conflict-free maneuvers of different aircraft. A maximum clique of minimum weight yields a conflict-free situation of minimal cost.

The advantage of this process is that it fully separates the modeling of aircraft dynamics, the separation verification and the costs computations from the resolution: whatever the hypotheses considered, and in particular taking into account uncertainties, the proposed mathematical framework will remain valid. The remainder of this section highlights the key elements of modeling and resolution of the model.

3.1 Graph construction

In this subsection, we introduce the *conflict graph* $\mathcal{G} = (\mathcal{V}, \mathcal{E})$ used to model the CR problem.

The set of vertices is defined as $\mathcal{V} = [\![1; |\mathcal{M}|]\!]$, where $\mathcal{M}$ denotes the set of possible maneuvers for all aircraft. We denote $\mathcal{V}_f$ the set of vertices corresponding to aircraft f.

Let $(i, j) \in \mathcal{V} \times \mathcal{V}$ be a pair of vertices representing maneuvers $(m_i, m_j) \in \mathcal{M} \times \mathcal{M}$ of aircraft $(f_i, f_j) \in \mathcal{F} \times \mathcal{F}$. For $i \neq j$, we write $m_i \square m_j$ when no conflict occurs if aircraft f_i follows maneuver m_i while aircraft f_j performs maneuver m_j. The set of edges $\mathcal{E}$ corresponds to the pairs of maneuvers performed by two different aircraft without creating conflicts:

$$\mathcal{E} = \left\{(i, j) \in \mathcal{V} \times \mathcal{V}, i \neq j : m_i \square m_j\right\} \tag{44}$$

Proposition 3.1(Lehouillier et al. (2015b)) links the cliques in $\mathcal{G}$ to the CR problem:

Proposition 3.1 *Let $\mathcal{C}$ be a clique in graph $\mathcal{G}$. Then $\mathcal{C}$ represents a set of conflict-free maneuvers for a subset of $\mathcal{F}$ of cardinality $|\mathcal{C}|$.*

For a more synthetic presentation, we consider in this subsection that maneuvers and vertices are equivalent without loss of generality. As explained in the previous subsection, the cost of a maneuver depends on its execution, which itself varies with the maneuvers of the other aircraft. As a consequence, we need to define the cost of the edges before the cost of the vertices.

Again, for ease of presentation, an edge $e = (i, j)$ is considered as a pair of maneuvers. We compute the cost of an edge $e = (i, j)$ as a pair constituted of the cost of maneuvers i and j, denoted $C_i^{(i,j)}$ and $C_j^{(i,j)}$.

Let us consider a maneuver i. The cost of each edge linking i to another maneuver j corresponds to an execution time t_i^j which is the minimum time during which i and j have to be executed before a safe return can be performed by at least one of the corresponding aircraft.

To determine the cost of i, denoted c_i, we need to compute the time t_i during which it is actually applied. If i is not in the optimal solution, then $t_i = 0$. Otherwise, t_i is given by

$$t_i = \max_{j \in \mathcal{V} \cap \mathcal{C}} t_i^j \tag{45}$$

Equation (45) states that maneuver i has to be applied long enough in order to be conflict-free with every other chosen maneuver. As a consequence, we can determine c_i:

$$c_i = \begin{cases} \max\limits_{j \in \mathcal{V} \cap \mathcal{C}} C_i^{(i,j)} & \text{if } i \in \mathcal{C} \\ 0 & \text{otherwise} \end{cases}$$

3.2 MILP formulation

In our model the costs of the vertices are not determined a priori, since they depend on which vertices are in the clique. As a consequence, the dedicated algorithms of existing graph theory libraries cannot be used in this study. To address this issue, we formulate our problem as a MILP that can be solved with any generic MILP solver.

The decision variables of the model all relate to the vertices of the graph. They correspond to the choice of the vertices in the clique and the cost of each vertex:

- $x_i = \begin{cases} 1 & \text{if vertex } i \text{ is part of the maximum clique} \\ 0 & \text{otherwise} \end{cases}$
- $c_i \in \mathbb{R}_+$ is the cost of vertex i.

The clique search can then be modeled as the following MILP, denoted MIP:

$$\text{minimize} \sum_{i \in \mathcal{V}} c_i \tag{46}$$

$$\text{subject to } x_i + x_j \leq 1, \forall (i,j) \in \mathcal{V} \times \mathcal{V} \setminus \mathcal{E} \tag{47}$$

$$\sum_{i \in \mathcal{V}} x_i = |\mathcal{F}| \tag{48}$$

$$c_i \geq C_i^{(i,j)}(x_i + x_j - 1), \forall (i,j) \in \mathcal{E} \tag{49}$$

$$x_i \in \{0;1\}, \forall i \in \mathcal{V} \tag{50}$$

$$c_i \geq 0, \forall i \in \mathcal{V} \tag{51}$$

The objective function (46) minimizes the cost of the maneuvers. Constraints (47) are clique constraints stating that two nonadjacent vertices must not be part of the clique. In terms of conflict resolution, it means that two maneuvers in conflict must not be part of the solution. Constraint (48) defines the cardinality of the maximum clique. Constraints (49) are used to compute the cost of the vertices: if a vertex is in the maximum clique, then its cost must be greater than the cost on every edge connecting it to other vertices in the clique. Otherwise, no particular constraint is imposed on the vertex cost. Constraints (50)–(51) are binarity and nonnegativity constraints, respectively.

3.3 Inserting uncertainties into the deterministic model

In this subsection, we explain how the expression of the probability of conflict between two aircraft derived in Subsection 2.6 is used to modify the deterministic model presented in this section.

An edge exists between two maneuvers if they are conflict-free. In other words, if the probability of conflict associated with these maneuvers is 0. If they are in conflict (i.e if the probability of conflict was 1), then no edge is drawn between the corresponding vertices. To take into account the uncertainties, we change the necessary condition to build an edge.

The set of edges $\mathcal{E}$ is defined by

$$\mathcal{E} = \{(i,j) \in \mathcal{V} \times \mathcal{V}, i \neq j : \mathbb{P}_c(i,j) < \delta_s\} \tag{52}$$

where δ_s is a security threshold restricting the set of possible maneuvers. δ_s represents an upper bound on the probability that a conflict remains after the maneuvers are issued. We remind here that a remaining conflict will always be solved: the controller will issue another set of maneuvers. In other words, δ_s can be regarded as an upper bound on the probability that the controller uses a recourse to solve the problem once again.

This adaptation of the deterministic setting makes a good pairing with the expression computed in Subsection 2.6. Indeed, when the set of possible maneuvers becomes very large, the number of probabilities to compute would require a huge computational effort if they were determined through simulation, whereas with our approach, we determine these values instantaneously.

4 Bi-Objective Optimization Procedure

In this section, we detail the bi-objective approach designed to solve the problem. This method optimizes the CR problem according to two criteria depicting the efficiency and the probability of having recourse related to a solution. It iteratively solves the model MIP according to the first criterion, while imposing a certain improvement on the second criterion between two consecutive resolutions. Each resolution results in a solution approximating the Pareto front of

the problem. In the end, the method provides the air traffic controller with a set of solutions corresponding to different trade-offs between efficiency and probability of using a recourse.

4.1 Optimization Criteria

The first criterion of optimization corresponds to the objective function of the mathematical program MIP presented in Section 3:

$$z_e = \sum_{i \in \mathcal{V}} c_i \tag{53}$$

This objective is the total amount of additional fuel burnt induced by the chosen maneuvers, and represents the aspect of a solution related to its economical efficiency. Indeed, it is an indicator on the perturbation of the planned trajectories and gives an insight into the effort required to catch up with the initial flight plan after the maneuver is performed. In addition to the perturbation of the set of aircraft itself, this criterion also illustrates the perturbation on surrounding traffic.

The second criterion is given by

$$z_s = \sum_{i \in \mathcal{V}} \sum_{\substack{j \in \mathcal{V} \\ j \neq i}} P_{ij} x_i x_j \tag{54}$$

where P_{ij} is the probability of conflict of maneuvers i and j, and x_i and x_j are the decision variables corresponding to whether or not maneuvers i and j are chosen. Value z_s corresponds to the expected number of conflicts potentially remaining after the solution is applied. This is a relevant measure for the controller as it gives an idea of the potential additional effort required to solve the problem once again in the close future. The higher z_s is, the higher the probability of re-issuing avoidance maneuvers will be. Variable z_s represents an indicator of the additional workload and cognitive charge that will potentially be required in order to definitely solve the problem.

To keep the expression of z_s linear in the decision variables, we apply Fortet's linearization Fortet (1960). We introduce a new set of binary variables y_{ij} respecting the following constraints:

$$y_{ij} \leq x_i, \forall i \in \mathcal{V}, \forall j \in \mathcal{V} \tag{55}$$

$$y_{ij} \leq x_j, \forall i \in \mathcal{V}, \forall j \in \mathcal{V} \tag{56}$$

$$y_{ij} \geq x_i + x_j - 1, \forall i \in \mathcal{V}, \forall j \in \mathcal{V} \tag{57}$$

$$\tag{58}$$

yielding a new expression of z_s.

$$z_s = \sum_{i \in \mathcal{V}} \sum_{j \in \mathcal{V}} P_{ij} y_{ij} \tag{59}$$

Algorithm 1 describes the mechanics of the iterative procedure. The user-defined parameters are the security threshold δ_s used to build the conflict graph, and an improvement thresholds δ_2 for the second criterion, respectively. The algorithm starts by solving the program MIP: it finds the optimal solution for the first criterion of value z_e. We compute z_s the value of this solution for the second criterion. The point (z_e, z_s) is a Pareto-optimal point, since it is globally optimal for the first criterion. The value of p is then used to add the constraint (60) to MIP:

$$\sum_{i \in \mathcal{V}} \sum_{j \in \mathcal{V}} P_{ij} y_{ij} \leq p - \delta_i \tag{60}$$

Constraint (60) simply reflects the minimum improvement required on the second criterion. The value of the parameter δ_i can be considered as a factor of granularity of the Pareto front. MIP is then solved once again, and the values of the two criteria are updated. The algorithm continues until the value of the second criteria becomes smaller than the threshold p_f.

Algorithm 1 Iterative bi-objective optimization procedure (IBIOP)

procedure IBIOP(δ_s, p_f, δ_i)
  Input: Set of aircraft $\mathcal{F}$, set of maneuvers $\mathcal{M}$
  Parameters: security thresholds δ_s, p_f , improvement threshold δ_i
  Build the conflict graph according to $\mathcal{F}$, $\mathcal{M}$ and δ_s
  $z_e \leftarrow +\infty$, $z_s \leftarrow +\infty$
  Solve MIP
  $z_e \leftarrow$ optimal value of MIP
  $z_s \leftarrow$ value of second criterion for optimal solution of MIP
  while $z_s \geq p_f$ **do**
    Add constraint $\sum_{i \in \mathcal{V}} \sum_{j \in \mathcal{V}} P_{ij} y_{ij} \leq p - \delta_i$ to MIP
    Solve MIP
    $z_e \leftarrow$ optimal value of MIP
    $z_s \leftarrow$ value of second criterion for optimal solution of MIP

5 Results

This section is organized as follows. Subsection 5.1 describes the values assigned to the different parameters for the experiments. Subsection 5.2 tests the validity of the assumptions made in the computations in Subsection 2.6. Computational results are detailed in Subsection 5.3. Subsection 5.4 provides a quantitative analysis of a Pareto front for a particular example.

5.1 Parameter values and simulations of the uncertainties distributions

In this subsection, we define the values assigned to the different parameters of the random variables distributions, and we describe the methods used to generate the random samples used for the Monte-Carlo simulations.

5.1.1 Parameter values of the uncertainties distributions.

We give the values assigned to the parameters of the distributions of the uncertainties.
Probability distribution of the wind: The simulated wind follows a zero-mean normal distribution of standard deviation $\sigma_{\mathbf{W}} = 5.4$kt, according to the model described in Chaloulos and Lygeros (2007).

Probability distribution of the error on speed prediction: We follow the model presented in Chaloulos and Lygeros (2007), where the error on speed prediction is a zero-mean normal variable of standard deviation $\sigma_{\mathrm{Y}} = 7.9$kt.

Probability distribution of the maneuver delays: As no data on these delays exist to our knowledge, we interviewed an experienced air traffic controller to obtain an insight into what those values could be. As a result, we decided to use the following values:

- $T^c + T^s \sim \mathcal{N}(\mu_{T^{c,s}}, \sigma_{T^{c,s}})$ where $\mu_{T^{c,s}} = 30$ seconds and $\sigma_{T^{c,s}} = 10$ seconds;

- $\forall i \in \mathcal{F}, T_i^p \sim \mathcal{N}(\mu_{T_i^p}, \sigma_{T_i^p})$ where $\mu_{T_i^p}$ is a random variable uniformly distributed between 20 and 40 seconds, and $\sigma_{T_i^p} = 10$ seconds;

5.1.2 Monte-Carlo simulations.

For the simulation of aircraft trajectories, we generate random values for the wind according to the method developed by Lymperopoulos (2010). The author performs a time and space discretization of the wind field, and iteratively computes at each time step the wind values at point of the grid according to the wind values computed at the previous time step, using correlation functions. The values of the normal distribution for the error on speed prediction and on the maneuver delay are generated according to the Box-Muller method described in Rubinstein and Kroese (2011), which simulates centered normal random variables using uniformly distributed random variables.

5.2 Validating the calculus through simulations

In this subsection, we validate the assumptions made in Subsection 2.6, by checking the validity of the approximation of the probability of conflict derived in Subsection 2.6 by comparing it to the probability obtained through simulations.

To this end, we study a test case representing a conflict situation with two aircraft i and j crossing each other with an angle θ (the set of values for theta is $\{60°; 90°; 120°\}$). To avoid the conflict, they start their maneuver at 100NM from the crossing point of their trajectories. We designed different scenarios corresponding to a couple of maneuvers (M_i, M_j) consisting in either speed or heading changes. The speed maneuvers range from -6% to 6% with a 1% step and the heading changes range from $-10°$ to $10°$ with a $1°$ step. In total, we have 545 scenarios. For each scenario, 2000 independent random samples are generated.

To validate the approximation of the probability of conflict derived in Subsection 2.6, for each scenario we computed the value of the approximated probability of conflict, and we simulated 2000 random scenario samples to estimate the probability of conflict. The same process was performed for the minimum distance between the two aircraft.

Configuration		Difference of separation distance		Difference of probabilities	
Maneuvers	Crossing angle (°)	Absolute Mean (NM)	Variance (NM)	Mean (%)	Variance
H/H	60	0.09	0.01	0.68	0.02
H/H	90	0.10	0.02	0.70	0.01
H/H	120	0.13	0.01	0.61	0.04
S/H	60	0.16	0.01	0.80	0.03
S/H	90	0.12	0.01	0.72	0.12
S/H	120	0.11	0.01	0.50	0.14
S/S	60	0.05	0.01	0.62	0.02
S/S	90	0.16	0.03	0.66	0.04
S/S	120	0.14	0.01	0.66	0.11

Table 1: Comparison of the simulation results and the calculus for the minimum distance and the probability of conflict

Table 1 highlights that the average simulated minimum distance is close to the computed one. Depending on the type of maneuver and the crossing angle, it ranges from 0.05 NM to

0.16 NM. The variance is really small, meaning that the difference between the two distances is usually close to the mean. Probabilities of conflict computed and simulated are almost identical, with a difference always under 1% for the considered instances, meaning that the expression derived in Subsection 2.6 is a really good approximation of the simulated probability.

Figure 5 highlights the results of Table 1 graphically, and focuses on two aircraft crossing with an angle of 90° and performing heading changes to avoid the conflict. Figure 5a compares the average of the computed distribution of the minimum distance with the average minimum distance simulated. Figure 5b compares the computed and simulated probability of conflict. Scenarios are sorted on the horizontal axis following decreasing values of the compared quantities. The plotted functions are stepwise, because the difference in maneuver magnitudes from one scenario to the other are discrete, which has a significant impact on the minimum distance and the resulting probability of conflict.

Figure 5: Comparison of calculus and simulations for two aircraft performing heading changes to avoid at the intersection of their planned trajectories making a 50° angle

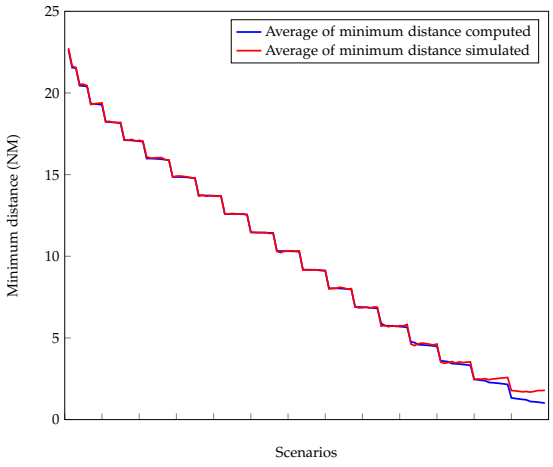

(a) Comparison of the average minimum distance simulated and the mean of the computed distribution of the minimum distance

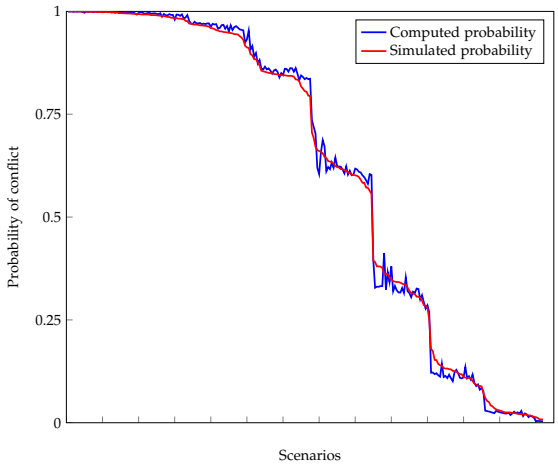

(b) Comparison of the computed and simulated probability of conflict

5.3 Computational results

5.3.1 Benchmark description

Structured benchmark. This benchmark gathers three types of instances. The first set is roundabout instances $\mathcal{R}_n$, where n aircraft are distributed on the circumference of a 100NM radius and fly towards the center at the same speed and altitude. The second set is crossing flow instances $\mathcal{F}_{n,\theta,d}$, where two trails of n aircraft separated by d nautical miles intersect each other with an angle θ. The last type of instance is a grid $\mathcal{G}_{n,d}$ constituted of two crossing flow instances $\mathcal{F}_{n,\frac{\pi}{2},d}$ with a 90° angle, one instance being translated 15NM North-East from the other. Aircraft considered for the conducted experiments are Airbus A-320 flying at 450 kt on flight level FL330. An example of these instances is given on Figure 6.

Random benchmark. This benchmark consists of random instances, where aircraft are uniformly distributed within a square sector with side length 50NM. To avoid generating infeasible instances, we perform a preprocessing before solving the problem: for each pair of aircraft that

Figure 6: Examples of instances of the benchmark

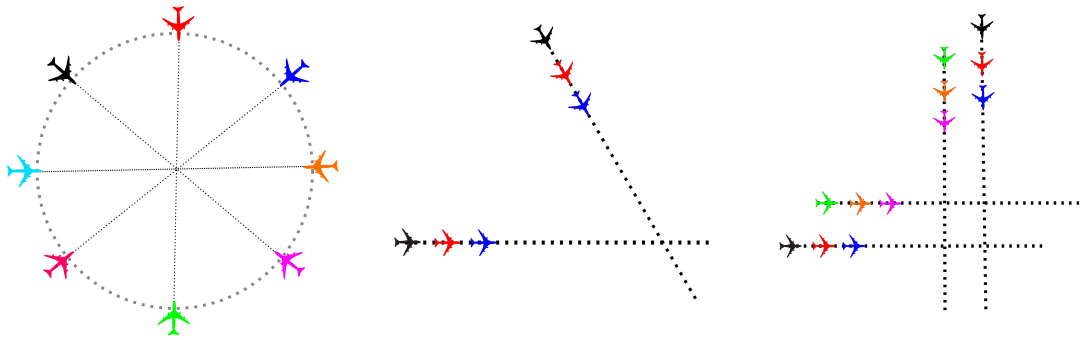

(a) Roundabout $\mathcal{R}_8$ (b) Crossing Flow $\mathcal{F}_{3,\frac{\pi}{4},10}$ (c) Grid $\mathcal{G}_{3,10}$

will loose separation within the first 30 seconds of observation, we randomly delete one of the aircraft. For a desired number of aircraft, we generate 15% more aircraft to anticipate the effect of the preprocessing. If more aircraft than desired remain after the preprocessing, extra aircraft are then randomly removed until the number is reached.

5.3.2 Computational results.

All tests were performed on a computer equipped with the following hardware: Intel Core i7-3770 processor, 3.4 GHz, 8-GB RAM. The algorithms were implemented in C++ and relies on CPLEX 12.5.1.0 CPL (2014) with default options to solve every instance. For instances with up to 10 aircraft, heading changes range from $-10°$ to $10°$ with a $2°$ step. For instances with more than 10 aircraft, the possible heading changes are $\pm 5°$, $\pm 10°$, $\pm 15°$ and $\pm 20°$. In addition, aircraft can also perform speed changes of $\pm 3\%$ and $\pm 6\%$. The parameters of the IBIOP procedure were assigned the following values:

- security threshold for a maneuver $\delta_s = 5\%$;
- improvement threshold for safety $\delta_i = 1\%$;
- the stopping criterion $p_f \leq 1\%$.

Table 2 gathers information about the instance dimensions, the generated solutions and computational results. The headings are given as follows:

- $|\mathcal{F}|$: number of aircraft;
- $|\mathcal{V}|$: number of vertices;
- $|\mathcal{E}|$: number of edges;
- 1^{sol} : first generated solution of the Pareto front, expressed as the pair (c_1, c_2) of the values of the two criteria, where c_1 is expressed in kilograms of fuel and c_2 is the expected number of conflicts;
- L^{sol} : last generated solution of the Pareto front, expressed as the pair (c_1, c_2) of the values of the two criteria, where c_1 is expressed in kilograms of fuel and c_2 is the expected number of conflicts;
- T^r : resolution time (in seconds);
- Nb^p : number of generated solutions of the Pareto front.

	Instance size			Solutions explored		Resolution	
	$\|\mathcal{F}\|$	$\|\mathcal{V}\|$	$\|\mathcal{E}\|$	1^{sol}	D^{sol}	T^r	Nb^p
$\mathcal{R}_4$	4	60	571	(12.26 ; 0.053)	(15.19 ; 0.005)	0.67	2
$\mathcal{R}_6$	6	90	1296	(32.12 ; 0.107)	(44.46 ; 0.009)	6.69	7
$\mathcal{R}_8$	8	120	2256	(77.04 ; 0.0917)	(100.7 ; 0.008)	8.58	8
$\mathcal{R}_{10}$	10	110	2647	(151.9 ; 0.072)	(252.3 ; 0.008)	11.69	5
$\mathcal{R}_{12}$	12	156	6215	(337.6 ; 0.184)	(370.3 ; 0.007)	24.17	4
$\mathcal{R}_{16}$	16	208	10924	(562.2 ; 0.137)	(914.8 ; 0.008)	139.7	11
$\mathcal{F}_{1,60,10}$	2	30	83	(5.85 ; 0.035)	(9.13 ; 0.001)	0.09	2
$\mathcal{F}_{2,60,10}$	4	60	717	(20.73 ; 0.037)	(21.79 ; 0.002)	1.26	2
$\mathcal{F}_{4,60,10}$	8	120	3543	(55.90 ; 0.045)	(59.48 ; 0.009)	7.46	2
$\mathcal{F}_{6,60,10}$	12	156	6027	(134.7 ; 0.023)	(137.6 ; 0.008)	42.92	2
$\mathcal{G}_{2,10}$	8	120	3690	(73.15 ; 0.078)	(90.20 ; 0.008)	30.9	5
$\mathcal{G}_{3,10}$	12	156	11034	(382.8 ; 0.020)	(480.1 ; 0.007)	82.89	4
$\mathcal{U}_{15}$	15	195	6940	(14.42 ; 0.0512)	(22.15 ; 0.002)	45.12	4
$\mathcal{U}_{25}$	25	325	12313	(65.07 ; 0.014)	(89.24 ; 0.004)	7.46	2
$\mathcal{U}_{35}$	35	455	33127	(89.15 ; 0.021)	(120.05 ; 0.009)	130.02	2

Table 2: Computational results

First, we observe that all the instances met the stopping criteria, yielding solutions with less than 0.01 expected conflicts. Results highlight that for instances with less than 10 aircraft, the solution time stays shorter than 30 seconds while on average 5 different solutions are generated. This achievement is meaningful for the air traffic controller, since he/she is able to access a small set of different solutions within a short period of time. For instances with more than 10 aircraft, solution times tend to slightly increase to reach up to two and a half minutes to generate 9 solutions (instance $\mathcal{R}_{16}$). Even though it seems far from real-time, the advantage of our procedure is that it generates solutions on the fly, meaning that the controllers has at least one or two possible solutions within the first seconds of the resolution if he/she needs to act quickly. Those solutions have a higher probability of using a recourse, but by concept it gives to the controller a certificate that at least each pair of aircraft has less than 5% chances of needing another avoidance maneuver in the future. An observation worth mentioning is that the total solution time is closely linked to the value of the security threshold δ_s and the stopping criterion. Indeed, their values will mostly influence the number of generated Pareto-front solutions. Moreover, for the experiments we choose to have a large set of possible maneuvers for each aircraft, which also has an impact on the solution time. A smaller set of maneuvers would result in a shorter execution time, especially if we delete the largest maneuvers, which represent the vertices with higher degrees. Indeed, those nodes have an impact on the number of cliques and on the search of a maximal clique of minimum weight.

5.4 Quantitative analysis of a solution set

We now focus on the solutions generated by our procedure applied to the instance depicted on Figure 7. One aircraft intersects a train of two aircraft separated by 20 NM. The algorithm parameters were identical to the ones for the other tests.

In order to get an insight into the effect of considering uncertainties on the chosen maneuvers, we remind that the deterministic solution is worth 5.54 kilograms of fuel. The generated solutions during the resolution are displayed on Figure 8. The first solution $(6.66; 0.35)$, was computed in 0.29 seconds. Every half second, a new solution is generated until the eighth and last one $(47.47; 0.009)$ which was computed in 6.22 seconds.

We can divide the generated solutions into two clusters, depending on their geometrical

Figure 7: Example for the analysis of the generated solutions

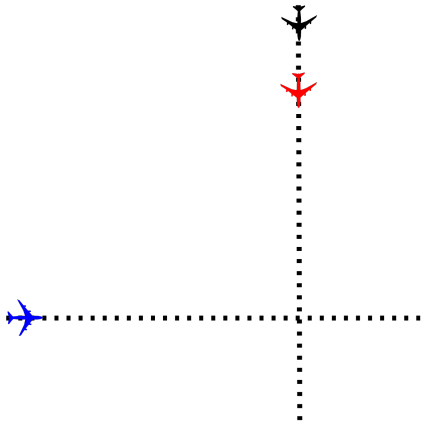

Figure 8: Generated Pareto solutions for instance $\mathcal{R}_8$

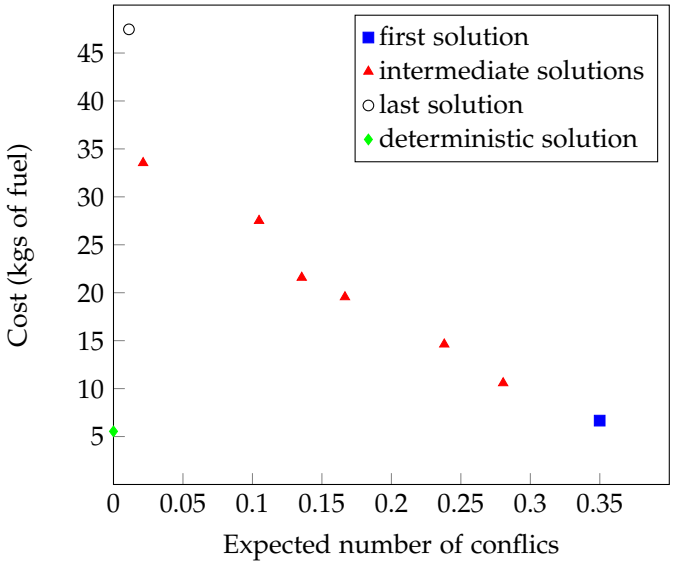

characteristics. The first cluster includes the first five generated solutions, where the blue aircraft flies between the two others, as evidenced on Figure 9a. Figure 9b describes the second cluster including the last three generated solutions. The blue aircraft performing a heading change, while the two others slow down.

The interpretations of these results are two-fold. First, it shows that there is a discontinuity in the geometry of the generated solutions, instead of having the same pattern repeated with a different magnitude. Second, it provides the controller with a visual outlook of the solutions, and he/she can easily identify which ones will be easier to communicate, or which ones will be the more robust.

Depending on the preferences of the controller, the quality of the solution will differ regarding one criterion or the other. For instance, if the controller aims at efficiency, he/she will apply the solution costing 6.66 kilograms of fuel, but where in 35% of the scenarios he/she will need to issue new maneuvers in order to ensure separation. If he/she aims at saving potential workload, he/she will choose a solution with less than 1% chances of having to re-issue maneuvers, but costing 47.47 kilograms of fuel. If his/her preferences are more mixed,

Figure 9: Two different geometrical solutions for the example

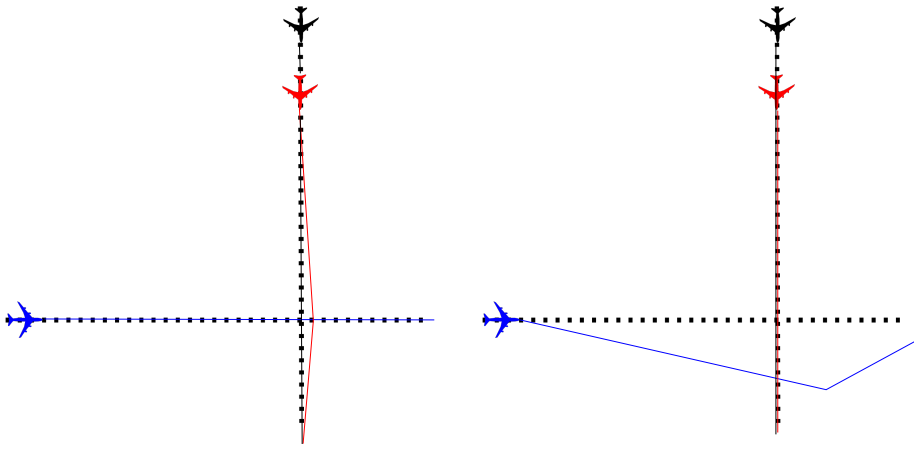

(a) First cluster (b) Second cluster

he/she still has six other possible solutions that he can choose.

6 Conclusions

In this article, we tackled the air conflict resolution problem under uncertainty. With our work, we provide the controller with a decision analysis tool generating a set of solutions representing different trade-offs between several criteria. The model is robust, since we consider a large span of uncertainties, including errors due to the wind, the imprecision of speed prediction. We also presented a new type of uncertainty: the delay in the execution of maneuvers. As a consequence, we cover a large part of the possible uncertainties that can arise during a conflict resolution. We computed the conflict probabilities and integrated them within an optimization model which is flexible, since it fully separates the modeling from the resolution process. Hence, the underlying mathematical framework remains valid, whatever the hypotheses considered. We focused on two objective that are relevant for conflict resolution, namely the extra fuel consumption, which serves as a performance index, and the expected number of conflicts, which serves as an indicator of potential additional workload required to re-issue avoidance maneuvers. We solve the problem by iteratively solving the aforementioned model, hence taking advantage of its power. Each resolution generates a solution of the Pareto front of the problem. At the end of the simulation run, the controller has a set of solutions where he can choose the one to apply, depending on the context and its preferences.

Monte-Carlo simulations validated the theory, and intensive simulations highlighted interesting results. Complex instances with up to 20 aircraft are solved within seconds, and an average of 5 different solutions are generated within two minutes.

Further research will focus on the extension of the method to aircraft with changing altitudes, in order to consider a bigger variety of problems. A rolling-horizon procedure will also be the center of new research, allowing us to run continuous simulations of real-life data sets.

Acknowledgement

This work was carried out under the project OPR-601 funded by the CRIAQ (Consortium on Research and Innovation in Aerospace in Quebec).

References

(2014). CPLEX v12.5. User's manual for CPLEX. Technical Report 11/03/08-08, IBM ILOG.

Alonso-Ayuso, A., Escudero, L. F., and Martin-Campo, F. J. (2012). A mixed 01 nonlinear optimization model and algorithmic approach for the collision avoidance in ATM: Velocity changes through a time horizon. *IEEE Transactions on Intelligent Transportation Systems*, 39:3136–3146.

Alonso-Ayuso, A., Escudero, L. F., and Martín-Campo, F. J. (2016). Multiobjective optimization for aircraft conflict resolution. a metaheuristic approach. *European Journal of Operational Research*, 248(2):691–702.

Archibald, J. K., Hill, J. C., Jepsen, N., Stirling, W. C., Frost, R. L., et al. (2008). A satisficing approach to aircraft conflict resolution. *IEEE Transactions on Systems, Man, and Cybernetics, Part C: Applications and Reviews*, 38(4):510–521.

Ballin, M. G. and Erzberger, H. (1996). *An analysis of landing rates and separations at the Dallas/Fort Worth International Airport*, volume 110397. Ames Research Center, National Aeronautics and Space Administration.

Chaloulos, G. and Lygeros, J. (2007). Effect of wind correlation on aircraft conflict probability. *Journal of Guidance, Control, and Dynamics*, 30(6):1742–1752.

Cole, R., Richard, C., Kim, S., and Bailey, D. (1998). Assessment of the Rapid Update Cycle (RUC) with near real-time aircraft reports. Technical report, MIT - Lincoln Laboratory.

Erzberger, H., Paielli, R. A., Isaacson, D. R., and Eshow, M. M. (1997). Conflict detection and resolution in the presence of prediction error. In *1st USA/Europe Air Traffic Management R&D Seminar, Saclay, France*, pages 17–20. Citeseer.

EUROCONTROL (2011). User manual for the Base of Aircraft Data (BADA). Technical report, Eurocontrol.

EUROCONTROL (2013). Eurocontrol long-term forecast: IFR flight movements 2013-2035. Technical report, Eurocontrol - STATFOR.

Fortet, R. (1960). Applications de lalgebre de Boole en recherche opérationelle. *Revue Française de Recherche Opérationelle*, 4(14):17–26.

Irvine, R. (2002). A geometrical approach to conflict probability estimation. *Air Traffic Control Quarterly*, 10(2):85–113.

Joint Planning and Development Office (2008). Next gen air transportation system integrated work plan, technical report. Technical report.

Lehouillier, T., Omer, J., Soumis, F., and Allignol, C. (2014). Interactions between operations and planning in air traffic control. *Proceedings of the 2nd International Conference of Research in Air Transportation, Istanbul*.

Lehouillier, T., Omer, J., Soumis, F., and Desaulniers, G. (2015a). A flexible framework for solving the air conflict detection and resolution problem using maximum cliques in a graph.

Lehouillier, T., Omer, J., Soumis, F., and Desaulniers, G. (2015b). A new variant of the minimum-weight maximum-cardinality clique problem to solve conflicts between aircraft. In Le Thi, H. A., Pham Dinh, T., and Nguyen, N. T., editors, *Modelling, Computation and Optimization in Information Systems and Management Sciences*, volume 359 of *Advances in Intelligent Systems and Computing*, pages 3–14. Springer International Publishing.

Lygeros, J. and Prandini, M. (2002). Aircraft and weather models for probabilistic collision avoidance in air traffic control. In *IEEE Conference on Decision and Control*, volume 3, pages 2427–2432. IEEE; 1998.

Lymperopoulos, I. (2010). *Sequential Monte Carlo methods in air traffic management*. PhD thesis, Diss., Eidgenössische Technische Hochschule ETH Zürich, Nr. 19004, 2010.

Martín-Campo, F.-J. (2010). *The collision avoidance problem: methods and algorithms*. PhD thesis.

Menon, P., Sweriduk, G., and Sridhar, B. (1999). Optimal strategies for free-flight air traffic conflict resolution. *Journal of Guidance, Control, and Dynamics*, 22(2):202–211.

Omer, J. (2015). A space-discretized mixed-integer linear model for air-conflict resolution with speed and heading maneuvers. *Computers & Operations Research*, 58:75–86.

Omer, J. and Farges, J.-L. (2013). Hybridization of nonlinear and mixed-integer linear programming for aircraft separation with trajectory recovery. *IEEE Transactions on Intelligent Transportation Systems*, 14(3):1218–1230.

Paielli, R. A. (2003). Modeling maneuver dynamics in air traffic conflict resolution. *Journal of Guidance, Control, and Dynamics*, 26(3):407–415.

Pallottino, L., Feron, E. M., and Bicchi, A. (2002). Conflict resolution problems for air traffic management systems solved with mixed integer programming. *IEEE Transactions on Intelligent Transportation Systems*, 3(1):3–11.

Prandini, M., Hu, J., Lygeros, J., and Sastry, S. (2000). A probabilistic approach to aircraft conflict detection. *IEEE Transactions on Intelligent Transportation Systems*, 1(4):199–220.

Rubinstein, R. Y. and Kroese, D. P. (2011). *Simulation and the Monte Carlo method*, volume 707. John Wiley & Sons.

Schwartz, B. E., Benjamin, S. G., Green, S. M., and Jardin, M. R. (2000). Accuracy of ruc-1 and ruc-2 wind and aircraft trajectory forecasts by comparison with acars observations. *Weather and Forecasting*, 15(3):313–326.

SESAR Joint Undertaking (2012). European ATM master plan, edition 2. Technical report.

Stirling, W. C. and Goodrich, M. A. (1999). Satisficing games. *Information Sciences*, 114(1):255–280.

Tomlin, C., Pappas, G. J., and Sastry, S. (1998). Conflict resolution for air traffic management: A study in multiagent hybrid systems. *IEEE Transactions on Automatic Control*, 43(4):509–521.